Bias error and its thermal drift due to fiber birefringence in interferometric fiber-optic gyroscopes

Junhao Liu[a,*], Yifan Liu[b], Tianhua Xu[b]

[a]Tianjin Institute of Electronic Materials, Department of Fiber-Optic Technology, Tianjin, China, 300220

[b]School of Engineering, University of Warwick, Coventry, United Kingdom, CV4 7AL

Abstract-Polarization-maintaining fibers (PMFs) with intrinsic highly stress-induced birefringence (SIB) are widely employed in interferometric fiber-optic gyroscopes (IFOGs). The performance of which is limited by the refractive index and its thermal fluctuations induced by the temperature variations. The SIB contributes to the refractive index variously along with the temperature. However, the bias error and its thermal drift arising from the SIB in PMFs are never considered. In this paper, we present theoretical analysis on high-performance IFOGs considering the effects of the SIB and its thermal fluctuation incorporated into the early model. The numerical analysis of the proposed model shows that the accuracy of IFOG using PMFs is better than single-mode fibers (SMFs) by a factor of 2,and the high performance with ultimate sensitivity of IFOGs is achievable by the special design of PMFs which depends not only on the pure Shupe effect but also on the effects from intrinsic SIB and its temperature sensitivity.

Keywords: Fiber-optic gyroscope, Bias error, Thermal drift, Stress-induced birefringence, Polarization-maintaining optical fiber.

*Corresponding author, E-mail address: deishi5204@163.com (Junhao Liu).

1. Introduction

The thermal drift in interferometric fiber-optic gyroscopes (IFOGs) has been extensively studied [1] since it was recognized by Shupe as a phase error from fiber-environment interactions [2]. The Shupe effect could be partly reduced by means of special material [3], the thermal isolation [4], and the symmetric winding technique of the coiling fiber [5-8] etc. The bias error, another error source in IFOGs, induced by the thermal stress through photo-elastic effect in SMFs [9,10], was verified by the simulations with the finite element method recently [11,12]. While the

bias error induced by the polarization coupling was investigated [13-15] for PMFs used in high performance IFOGs [16,17], the effect of stress-induced birefringence (SIB) produced by the stress-applying parts (SAPs) in PMFs were not considered in the previous reports. As a result, the influence of employing PMFs on the performance of IFOGs becomes unclear, leaving the resultant effect due to the phase error of SIB and its thermal fluctuation unanalyzed. In fact, it is the thermal stress from SAPs that produces SIB in PMFs by the photo-elastic effect, which results in a changed refractive index [18-20]. Meanwhile, the SIB varies with temperature in PMFs [21-26], and the temperature-induced refractive index fluctuations could influence the thermal drift [2] and the bias error [27] in IFOGs. The phase variation induced by temperature has already been investigated for SMFs [28-34] and PMFs [35, 36], especially the thermal coefficient of SIB in PMFs [37-41]. Experimental results from previous studies can be directly applied to estimate the phase error in IFOG using PMFs. In this work, we incorporate the phase error originated from SIB in PMFs into the SMF model. Comprehensive analyses of the impact of the photo-elastic effect, the intrinsic high stress-induced birefringence, the thermal drift due to the SIB and the Shupe effect are performed in detail.

2. Theoretical model

An IFOG is a Sagnac interferometer based on sensing coils composed of optical fibers [1]. As shown in Fig. 1, a set of sensing coils with mean diameter D, thickness d and height h is wound by optical fibers with the effective refractive index of n_{eff} and the

thermal expanding coefficient of α in the core area. At the position of coordinate l along the fiber length L, the gyro bias $\Omega(t)$ induced by time-varying temperature rate $\dot{T}(l,t)$ of the local temperature $T(l,t)$ could be written as [2]

$$\Omega(t)=\frac{n_{\text{eff}}^2}{DL}\left(\frac{\mathrm{d}\phi}{\phi \mathrm{d}T}\right)\int_0^L \dot{T}(l,t)\left(L-2l\right)\mathrm{d}l, \tag{1}$$

where $\phi = kn_{\text{eff}}L$ is the propagation phase, and its temperature derivative $\mathrm{d}\phi/\mathrm{d}T$ is

$$\frac{\mathrm{d}\phi}{\mathrm{d}T}=k\left(n_{\text{eff}}\frac{\mathrm{d}L}{\mathrm{d}T}+L\frac{\mathrm{d}n_{\text{eff}}}{\mathrm{d}T}\right). \tag{2}$$

Normally, for fibers under normal temperature range from 230K to 330K, we can take the derivative of temperature from the phase temperature sensitivity $\Delta\phi/\phi\Delta T$ in early works [30] as an approximation:

$$\frac{\Delta\phi}{\phi\Delta T}=\frac{1}{n}\frac{\partial n}{\partial T}+\frac{1}{\Delta T}\left\{\varepsilon_z-\frac{n^2}{2}\left[\left(p_{11}+p_{12}\right)\varepsilon_r+p_{12}\varepsilon_z\right]\right\}. \tag{3}$$

FromEq.(1)-Eq.(3) it can be concluded as follows

$$\Omega(t)=\frac{n_{\text{eff}}}{DL}\cdot\left(\alpha n_{\text{eff}}+\frac{\mathrm{d}n_{\text{M}}}{\mathrm{d}T}+n_{\text{M}}\left[\left(1-\frac{n_{\text{M}}^2}{2}p_{12}\right)\frac{\mathrm{d}\varepsilon_z}{\mathrm{d}T}-\left(\frac{n_{\text{M}}^2}{2}\right)\left(p_{11}+p_{12}\right)\frac{\mathrm{d}\varepsilon_r}{\mathrm{d}T}\right]\right)\cdot\int_0^L \dot{T}(l,t)\left(L-2l\right)\mathrm{d}l$$

, (4)

where n_{M} is the refractive index of the core material itself, ε_z and ε_r are longitudinal and transverse thermal strain, and p_{11} and p_{12} are Pockel's coefficients of the core material. The fact that Eq. (4) turns out to be exactly the same as the model for SMFs in early works [1, 2, 9-12] confirms the correct use of Eq. (1) for the proposed model. However, the derivation of the Eq. (1) is not constrained to IFOGs using SMFs. It could also be used to calculate the bias of IFOGs with sensing coil wound by PMFs regarding which more details are illustrated in Section 3.

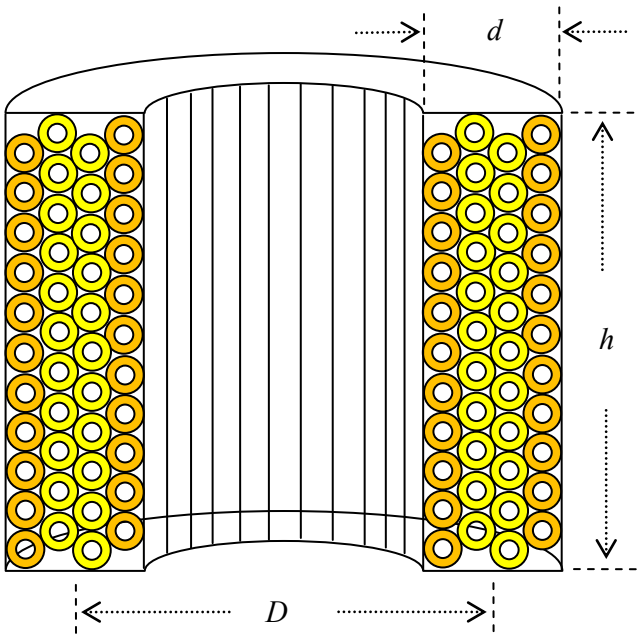

Fig.1 Structure of the fiber coils for I-FOGs

As a numerical example throughout the paper, we have compared the output biases of IFOGs using different types of sensing coils, SMFs and PMFs respectively, with the same scheme. The parameters of the fiber coils are listed in Table 1. The fiber length $L = 3770\,\mathrm{m}$, the number of layers $N_L = 64$, the number of turns per layer $N_N = 125$, total number of turns $N = 8000$, and the mean diameter $D = 150\,\mathrm{cm}$. For an optical wavelength $\lambda = 1550\,\mathrm{nm}$, the effective refractive index is $n_\mathrm{M} = 1.444268$ [42]. According to Shupe [2], Eq. (1) can be rewritten into Eq. (5) as an approximation

$$\Omega(t) \approx \frac{L n_\mathrm{M} \Delta T}{6D}\left(n_\mathrm{M}\frac{\mathrm{d}\phi}{\phi \mathrm{d}T}\right). \tag{5}$$

After taking $\left(\mathrm{d}\phi/\phi\mathrm{d}T\right)_\mathrm{SMF} = 1.64\times10^{-5}$ /K for SMFs [30], a gyro bias of $\Omega_\mathrm{SMF} = 0.0821$ deg/h for one hour mission time and temperature uniformity $\Delta T = 0.01\,\mathrm{K}$ can be derived.

Table 1 The parameters of fiber coil in typical IFOGs with high performance

Parameter	Mean diameter	Layers	Turns per layer	Total turns	Length
Symbol	D	N_L	N_N	N	L
Unit	cm	1	1	1	m
value	150	64	125	8000	3770

3. Verification and Analysis

Based on the temperature derivative of phase in Eq.(2), the model Eq. (1) for Shupe effect can be rewritten as:

$$\Omega(t)=\frac{n_{\text{eff}}}{DL}\left(\alpha n_{\text{eff}}+\frac{\mathrm{d}n_{\text{eff}}}{\mathrm{d}T}\right)\cdot\int_0^L\dot{T}(l,t)\left(L-2l\right)\mathrm{d}l, \tag{6}$$

where the effective refractive index n_{eff} is [9-12]

$$n_{\text{eff}}=n_{\text{M}}+n_{\text{P-E}}, \tag{7}$$

here $n_{\text{P-E}}$ is the refractive index increment induced by coating material through the photo-elastic effect under increasing temperature.

For the SMF transverse structure shown in Fig.2(a), the refractive index increment $n_{\text{P-E}}^{\text{SMF}}$ equals to the increment $n_{\text{P-E}}^{\text{Coatings}}$ induced by fiber coatings through thermal photo-elastic effect, which is half of the birefringence B_{SMF} in SMFs i.e.:

$$n_{\text{P-E}}^{\text{SMF}}=n_{\text{P-E}}^{\text{Coatings}}=B_{\text{SMF}}/2. \tag{8}$$

Here $B_{\text{SMF}}>0$ and $\mathrm{d}B_{\text{SMF}}/\mathrm{d}T>0$ comes from the compress (negative) stress of coatings and its increment when the fiber is heated up.

In terms of the one with PMF shown in Fig.2(b), the refractive index increment $n_{\text{P-E}}^{\text{PMF}}$ equals to the increment induced by both coatings and SAPs that is half of the birefringence B_{PMF} in PMFs:

$$n_{\text{P-E}}^{\text{PMF}} = n_{\text{P-E}}^{\text{Coatings}} + n_{\text{P-E}}^{\text{SAPs}} = B_{\text{SMF}}/2 + B_{\text{SAP}}/2 = B_{\text{PMF}}/2. \tag{9}$$

Here $B_{\text{PMF}} < 0$ and $\mathrm{d}B_{\text{PMF}}/\mathrm{d}T < 0$ comes from the tensile (positive) stress induced by SAPs and its decrement when the fiber is heated up. Then, after containing the birefringence effect, the thermal drift in I-FOGs with SMFs and PMFs can be written as

$$\begin{aligned}\Omega(t) &= \Omega_{\text{Shupe}}(t) + \Omega_B(t) \\ &= \frac{n_{\text{eff}}}{DL}\cdot\left(\alpha n_{\text{eff}} + \frac{\mathrm{d}n_{\text{M}}}{\mathrm{d}T} + \frac{1}{2}\frac{\mathrm{d}B}{\mathrm{d}T}\right)\cdot\int_0^L \dot{T}(l,t)\left(L-2l\right)\mathrm{d}l'\end{aligned} \tag{10}$$

where the birefringence B should be considered as Eq.(8) for SMFs (an increment in positive birefringence) and Eq.(9) for PMFs (a decrement in negative birefringence).Again, Eq. (10) can be simply evaluated as

$$\Omega(t) \approx \frac{Ln_{\text{eff}}\Delta T}{6D}\cdot\left(\alpha n_{\text{eff}} + \frac{\mathrm{d}n_{\text{M}}}{\mathrm{d}T} + \frac{1}{2}\frac{\mathrm{d}B}{\mathrm{d}T}\right), \tag{11}$$

for the temperature uniformity ΔT. These are consistent with previous works when using Eq.(7) and Eq.(8) for SMFs [9-12].For the gyro bias $\Omega_{\text{SMF}} = 0.0821\,\text{deg/h}$ in the example mentioned above, given the thermal expansion $\alpha = 0.055\times10^{-5}$/K and thermal coefficient of index $\mathrm{d}n_{\text{M}}/\mathrm{d}T = 0.7\times10^{-5}$/K [42], the refractive index increment induced by fiber coating through photo-elastic effect during temperature rise is then derived as $\mathrm{d}n_{\text{P-E}}^{\text{Coatings}}/\mathrm{d}T = 0.885\times10^{-5}$/K, which makes an agreement with the thermal drift for a gyro using SMFs, and is considered the dominant component out of the three error sources.

Equation (10) contains three terms that could induce the phase error. The first term is the thermal expansion αn_{eff} of the effective refractive index. The second term is the thermal variation $\mathrm{d}n_{\text{M}}/\mathrm{d}T$ of the material refractive index. These two terms illustrate the pure Shupe effect in SMFs [1,2]. The third term, $\mathrm{d}B/2\mathrm{d}T$, is the one induced by the photo-elastic effect when SMFs undergo temperature increasing [9-12]. That is to say, the third term represents the thermal induced birefringence in SMFs.

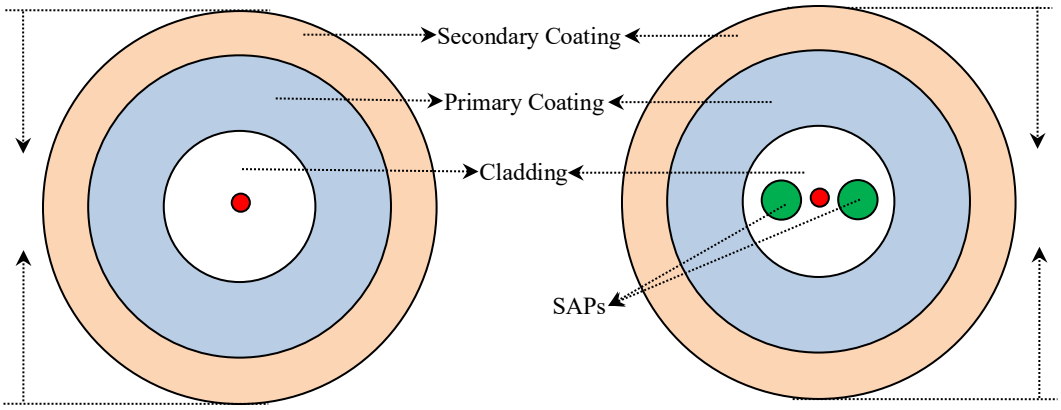

(a) (b)

Fig.2 Transverse structures of (a) SMF and (b) PMF

In order to validate Eq. (10) for PMFs, the following Eq. (12) should hold:

$$n_{\text{eff}}\frac{\mathrm{d}\phi}{\phi\mathrm{d}T}=\alpha n_{\text{eff}}+\frac{\mathrm{d}n_{\text{M}}}{\mathrm{d}T}+\frac{1}{2}\frac{\mathrm{d}B}{\mathrm{d}T}, \tag{12}$$

which can be easily obtained for $n_{\text{eff}}=n_{\text{M}}+B_{\text{PMF}}/2$ and $\phi=n_{\text{eff}}kL$ in PMFs. Equation (10) is thus valid for IFOGs with sensing coil wound by both SMFs and PMFs, provided that Eq.(8) and Eq.(9) are selected for effective refractive index of SMFs and PMFs. Table 2 lists the thermal drift components $\Omega_B(t)$ which comes from the

fiber birefringence for the coils with various fiber types underthe same configuration from example above (Table 1).

Table 2 Thermal drifts in IFOGs with different types of sensing fibers under the same coil configuration

Parameter	SMF	Panda PMF	Tiger PMF	Bowtie PMF	Holy PMF
α	5.5×10^{-7}	5.5×10^{-7}	5.5×10^{-7}	5.5×10^{-7}	5.5×10^{-7}
$\mathrm{d}n_{\mathrm{M}}/\mathrm{d}T$	7×10^{-6}	7×10^{-6}	7×10^{-6}	7×10^{-6}	7×10^{-6}
$\Omega_{\mathrm{Shupe}}(t)$	3.78×10^{-2}	3.78×10^{-2}	3.78×10^{-2}	3.78×10^{-2}	3.78×10^{-2}
B	0	5×10^{-4}	5×10^{-4}	5×10^{-4}	3.55×10^{-4}
$\mathrm{d}B/\mathrm{d}T$	8.9×10^{-6}	-5.93×10^{-7}	-5.36×10^{-7}	-5.29×10^{-7}	-3.31×10^{-9}
$\Omega_B(t)$	4.43×10^{-2}	2.97×10^{-3}	2.68×10^{-3}	2.65×10^{-3}	1.66×10^{-5}
$\Omega(t)$	8.21×10^{-2}	4.08×10^{-2}	4.05×10^{-2}	4.04×10^{-2}	3.78×10^{-2}

The results of four types of PMFs listed in Table 2 show that the performance improvement of IFOG by using PMFs rather than SMFs is not as significant as the effect of the thermal coefficients of their birefringence brings. That is because the common dominant component in both cases is the thermal coefficient of refractive index, i.e. $\mathrm{d}n_{\mathrm{M}}/\mathrm{d}T$ ($\sim7\times10^{-6}$ 1/K). It nearly equals the thermal coefficient of birefringence in SMFs ($\sim8.9\times10^{-6}$ 1/K), and is two orders of magnitude higher than the thermal expansion in PMFs ($\sim5.5\times10^{-7}$ 1/K).Therefore, the main purpose of using PMFs in IFOGs is to prevent the temperature-induced birefringence from fiber coatings by its intrinsic birefringence ($\sim5\times10^{-4}$), which is exactly the photo-elastic effect investigated in early works [9-11].

Another result from Table 2thatgives the better thermal drift in IFOGs comes from better thermal stability of the fiber birefringence. The thermal drift in IFOGs using PMFs will achieve a better resultant with a specific birefringence and its temperature stability, which calls for a special design of PMFs. The design can be attributed to the normalized temperature sensitivity H of PMFs [24] as the following.

For normal temperature range, thermal coefficient $\mathrm{d}B/\mathrm{d}T$ of the birefringence in PMFs can be obtained from the temperature sensitivity $\Delta B/B\Delta T$ of the birefringence defined in [24]: $\Delta B/B\Delta T = H/T_{\mathrm{d}}$,which gives $\mathrm{d}B/\mathrm{d}T = BH/T_{\mathrm{d}} = -\lambda H/\Lambda T_{\mathrm{d}}$. Here $T_{\mathrm{d}} > 0$ is the difference between the ambient temperature and the fictive temperature of SAPs in PMFs, $B = -\lambda/\Lambda < 0$is modal birefringence of the fiber (Λ is polarization beat length of the fiber), and H is the normalized temperature sensitivity of the modal birefringence [24].

The analytical expression for the thermal drift in I-FOGs with PMFs can be therefore obtained as:

$$\Omega(t) = \frac{n_{\mathrm{eff}}}{DL} \cdot \left(\alpha n_{\mathrm{eff}} + \frac{\mathrm{d}n_{\mathrm{M}}}{\mathrm{d}T} + \frac{\lambda H}{2\Lambda T_{\mathrm{d}}} \right) \cdot \int_0^L \dot{T}(l,t)\left(L - 2l\right)\mathrm{d}l, \tag{13}$$

where Λ is the polarization beat length of the fiber.

From Eq. (13), one of the ways to get better I-FOGs is to minimize the parameter

$$\Delta = \alpha n_{\mathrm{eff}} + \frac{\mathrm{d}n_{\mathrm{M}}}{\mathrm{d}T} + \frac{\lambda H}{2\Lambda T_{\mathrm{d}}}, \tag{14}$$

which dominates the thermal drift in IFOGs. For the normal temperature uniformity (ΔT =0.01 K) and the same coil design (Table 1), the best commercial PMF

(polarization beat length $\Lambda = 2.0$ mm at $\lambda = 1550$ nm and normalized temperature sensitivity $H = 1$ and $T_{\mathrm{d}} = 1000\,\mathrm{K}$) could achieve a thermal drift of 0.0397 deg/h when $\Delta = 7.55\times10^{-6}/\mathrm{K}$ without any compensation. The further work should focus on the compensation of the parameters for PMFs in Eq. (14) to improve the performance of I-FOGs, especially the normalized temperature sensitivity H. The first two terms can be feasibly compensated because of their linearity with temperature in normal range, and the birefringence term ($\lambda H/2\Lambda T_{\mathrm{d}} = \left|\mathrm{d}B/\mathrm{d}T\right| = 3.87\times10^{-7}$) leaves a drift of 0.0019 deg/h for the coil scheme of Table 1 and the best commercial PMF with a complete compensation of the pure Shupe effect. Now a new compensation of the birefringence fluctuation is necessary for a further improvement. The main difficulty for the new compensation lies in the variety and instability of the normalized temperature sensitivity in PMFs [24].

4. Numerical Estimation

The rate of temperature changing in sensing fibers is essential to accurately calculate the thermal drift in Eq. (10). Using the model developed by Mohr and the coordinate transformation between the radial direction in fiber coil and the circumferential direction in coiling fiber, the thermal drift in IFOGs with a quadrupole fiber coil can be described as [6]

$$\begin{aligned}\Omega(t) = {} & n_{\mathrm{eff}}\cdot R\cdot P\cdot\left(\frac{L}{D}\right)\cdot\left(\frac{1+N_L}{N_L^2}\right)\cdot\left(\alpha n_{\mathrm{eff}}+\frac{\mathrm{d}n_{\mathrm{M}}}{\mathrm{d}T}+\frac{\mathrm{d}B}{2\mathrm{d}T}\right)\\ & \cdot\exp\left(-\frac{t}{S}\right)\cdot\sum_{u=1}^{N_L}\left\{\left[Y_1(q_u,t)+Y_2(q_u,t)\right]\cdot\left[1-\frac{2u}{1+N_L}\right]\right\},\end{aligned} \tag{15}$$

where P is the thermal power of thermal source, q_u is the radical coordinates in each layer and u is the coordinates of the layer, N_L is the number of layers in fiber coil, and Y_1 and Y_2 are exactly the same as in [6]:

$$Y_1(q,t)=\frac{1}{a\sqrt{\pi t}}\cdot\exp\left(-\frac{k_1^2}{2t}\right)-\exp\left(ak_1+a^2t\right)\cdot\operatorname{erfc}\left(\frac{k_1}{2t}+at\right)$$

$$Y_2(q,t)=\frac{1+4a^2t}{a\sqrt{\pi t}}\cdot\exp\left(-\frac{k_2^2}{2t}\right)-\left[3(1+ak_2)+4a^2t\right]\cdot\exp\left(ak_2+a^2t\right)\cdot\operatorname{erfc}\left(\frac{k_2}{2t}+at\right), \tag{16}$$

and

$$a=\frac{1}{RQ}\sqrt{\frac{1}{\rho bC}},\quad S=\rho CQR',\quad k_1=\frac{q}{d}\sqrt{\frac{\rho C}{b}},\quad k_2=\frac{2d-q}{d}\sqrt{\frac{\rho C}{b}},\quad \operatorname{erfc}(x)=\frac{2}{\sqrt{\pi}}\int_x^{\infty}e^{-x^2}\mathrm{d}x$$

. (17)

where Q is the cross-sectional area, R is the heat radiating resistance, R' is the heat conductive resistance, C is the specific heat, b is the thermal conductivity, ρ is the density and d is the thickness.

Bias error in Eq. (13) for IFOGs with a quadrupole fiber coil composed of SMFs or PMFs can be directly calculated with the values of all the related parameters provided. The following numerical calculations are based on the same coil scheme (Table 1) for a typical high performance IFOG. The remaining parameters values are: conductivity $b=0.34$ W/(m·K), specific heat $C=1.427$ W/(g·K), and density $\rho=1504\,\mathrm{kg/m^3}$in SMFs and PMFs for simplicity [6]. The thermal power is $P=3$ Wand the difference between the fictive temperature and the ambient temperature of SAPs is $T_\mathrm{d}=1000\,\mathrm{K}$ for PMFs.

Figure 3 shows the three componential and the total bias and its thermal drift of an IFOG with a sensing coil wound by a SMF. The solid curve indicates the total gyro

bias, and the three dashed curves represent the bias induced by each component of phase perturbation in the SMF. The minimum contribution comes from the linear expansion of the fiber length, the maximum is induced by the thermally induced photo-elastic effect (birefringence in SMF) and the thermal coefficient of the refractive index for core material contributes to total bias intermediately.

The thermal drift (0.09 deg/h) of the IFOG shown in Fig.3 is higher than the estimation value 0.082 deg/h from Eq. (5) as the latter simplifies the integration by assuming the temperature uniformity. The numerical calculation in Eq. (15) has considered the thermal properties of the sensing coils by the relevant parameters and the sum based on the quadrupole pattern. The estimation is fast and simple, and the calculation is complete and accurate.

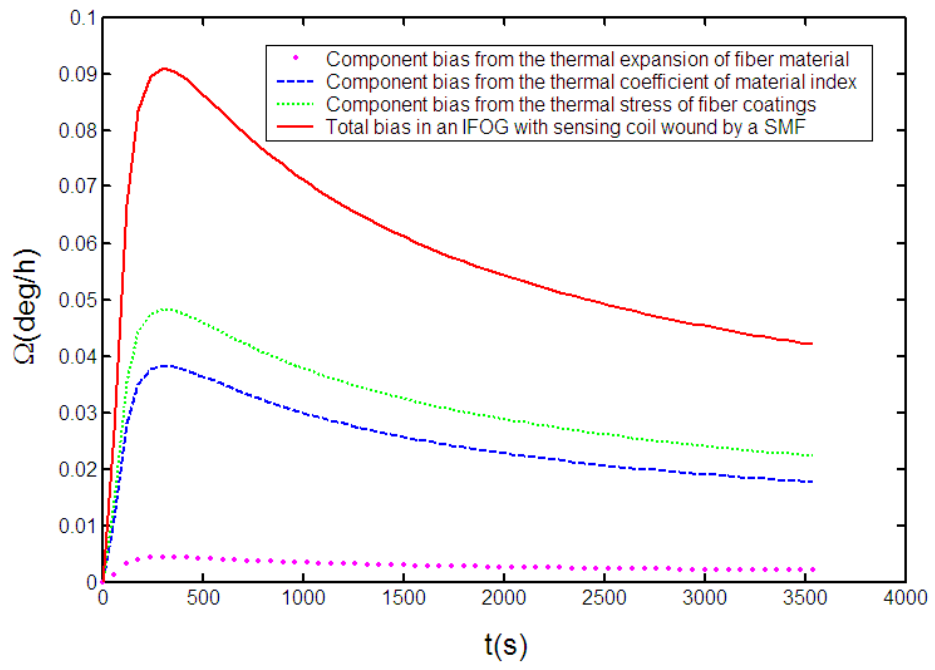

Fig.3 The thermal drift induced by each component of phase perturbations of an typical high-performance IFOG with an quadrupole sensing coil wound

Another fact shown in Fig. 3 is that the peak value of the thermal drift occurs at the same time for each component. It is the characteristic time [1] given by $\tau = \rho dC/2b$, which is a constant 315s for the thermal parameters in this work.

Figure 4 shows gyro bias of four modal birefringence of PMFs in commercial use where its normalized temperature sensitivity is in unit i.e. $H = 1$. For common PMFs (wavelength $\lambda \sim 10^{-6}$ m and beat length $\Lambda \sim 10^{-3}$ m or $B \sim -10^{-5}$), there is $\lambda H/\Lambda T_{\mathrm{d}} \sim 10^{-7}$ 1/K for $T_{\mathrm{d}} \sim 10^{-3}$ K which is consistent with the measurement of $\mathrm{d}B/\mathrm{d}T$ for PMFs [36-40]. Therefore, $\Delta > 0$ always holds since the material expansion ($\alpha n_{\mathrm{eff}} > 0$) and the thermal coefficient of refractive index ($\mathrm{d}n_{\mathrm{M}}/\mathrm{d}T > 0$) are both positive. It is of interest that a higher birefringence (i.e., shorter beat length) brings a higher drift. That is the very characteristic of the negative birefringence in PMFs. It is straight from Eq. (13) that a shorter beat length carries a higher increment in errors. Another fact showed in Fig. 4 is that the bias error from commercial PMFs of different birefringence are very close to each other. The differences among them are reduced about 1000 times by the temperature difference T_{d}. It should be noticed that all above are based on the negative birefringence ($B < 0$) and its positive normalized temperature sensitivity ($H > 0$) in PMFs. It is clear that a higher temperature sensitivity corresponds to a worse drift in this range, as shown in Fig. 5.

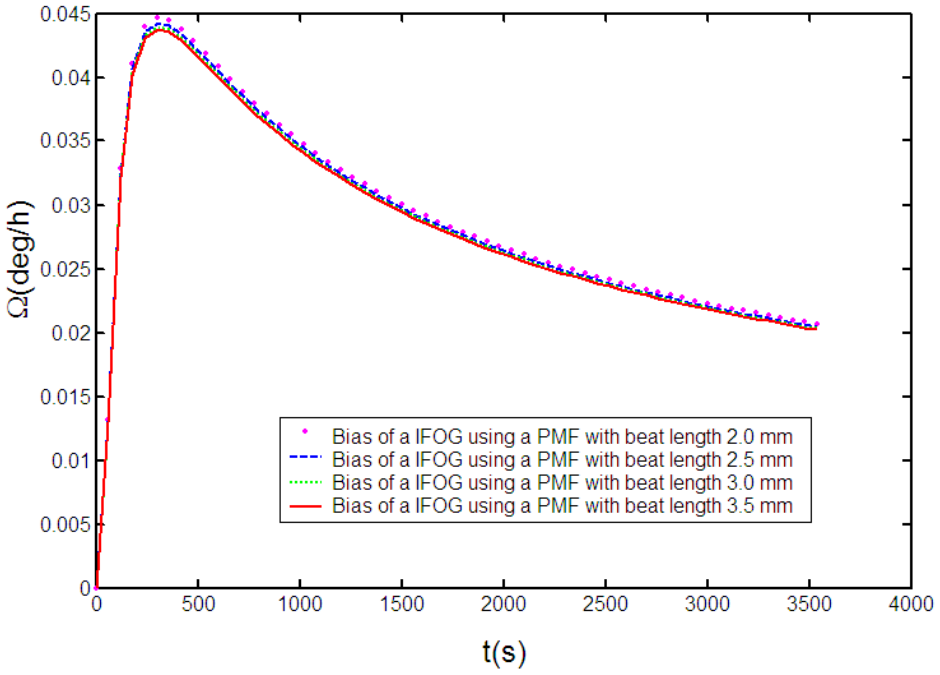

Fig.4 The thermal drift of I-FOGs with a quadrupole sensing coil wound by PMFs with different birefringence for unit normalized temperature sensitivity.

Figure 5 shows gyro bias of four normalized temperature sensitivities in ordinary commercial PMFs [24]. As expected, the drift and the normalized temperature sensitivity (H) share the same tendency i.e. higher H brings more significant drift in the normal range of $B<0$ and $H>0$.

Comparing Fig. 3 and Fig. 4, for the same coil scheme as listed in Table 1, the thermal drift of IFOG using PMF is about half of that of SMF. This is an advantage of PMF over SMF apart from the cross coupling of orthogonal polarization. It is natural to raise the question: how the thermal drift could be further improved. A theoretical solution is to add a compensation term in Eq. (14) to achieve $\Delta=0$ indicating the complete cancelation of the phase errors. Actually, the birefringence term could be a compensative term if the normalized temperature sensitivity is negative ($H<0$),

which occurs for the special fiber design [24]. Then it will occur on the condition of $H = -2\Lambda T_{\mathrm{d}}\left(\alpha n_{\mathrm{M}} + \mathrm{d}n_{\mathrm{M}}/\mathrm{d}T\right)/\lambda$, which is $H \approx -30.1717$ for PMFs with $\Lambda = 3.0\,\mathrm{mm}$. This optimum H value depends on a few parameters (Λ , T_{d} , α , n_{M} , λ)and is independent to other parameters (b , C , ρ , d_0 , D , L , N_N , N_L , R , P , etc).

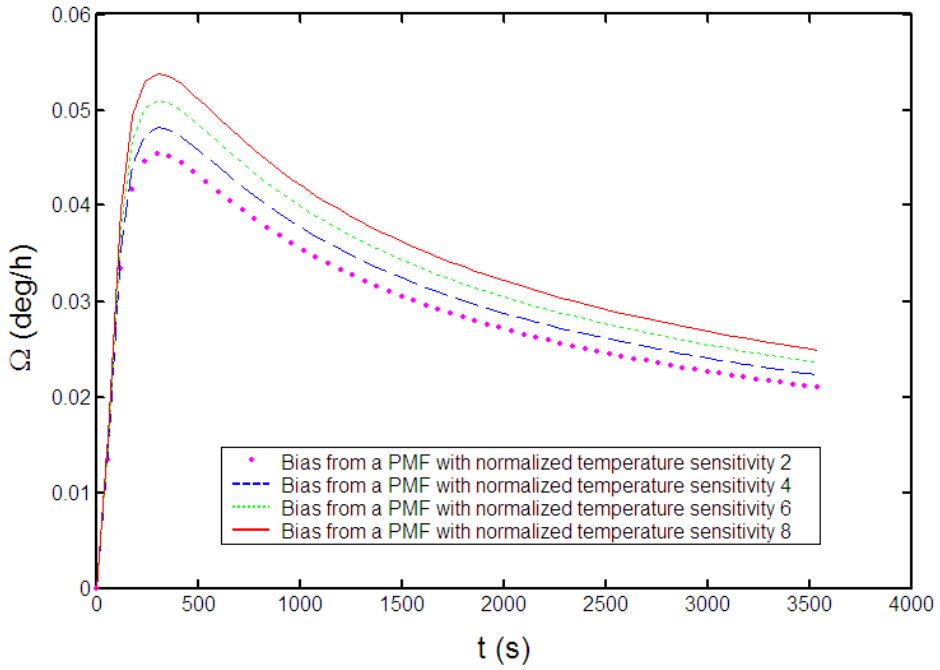

Fig.5 The thermal drift of I-FOGs with a quadrupole sensing coil wound by PMFs with different normalized temperature sensitivity of birefringence for constant birefringence.

As shown in Fig.6, when the magnitude of the special designed birefringence term $H = -2\Lambda T_{\mathrm{d}}\left(\alpha n_{\mathrm{M}} + \mathrm{d}n_{\mathrm{M}}/\mathrm{d}T\right)/\lambda$ covers the pure Shupe error, i.e., the phase error induced by the thermal expansion of fiber length and the temperature coefficient of the material refractive index, the total drift could be improve further. The H value in Fig. 6 is to show our requirement when the birefringence term is used as a unique compensation. Another method can be applied at the same time in practice to get the H value [24].

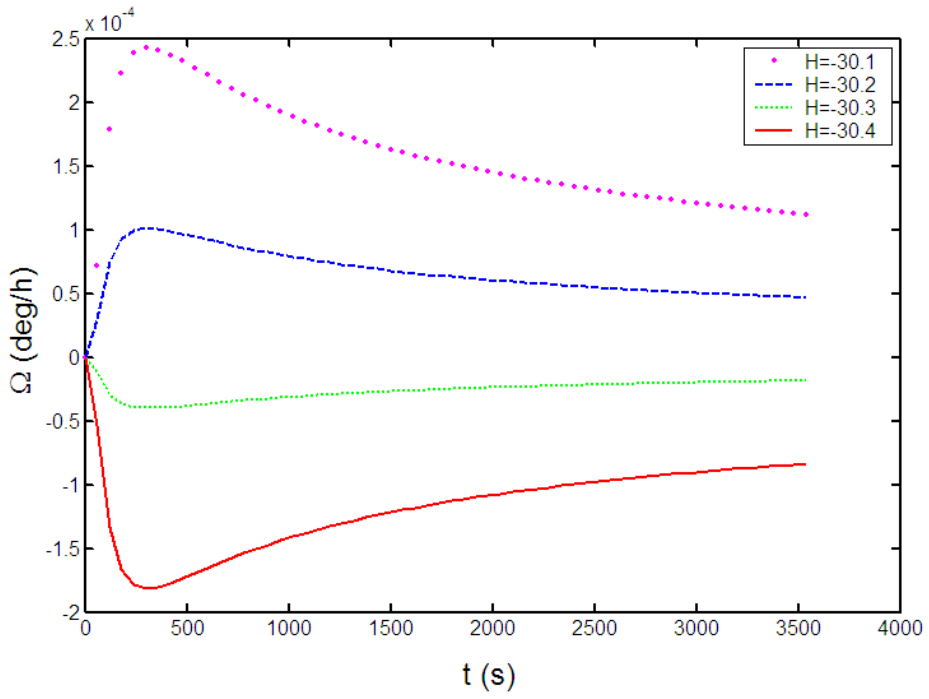

Fig.6 The thermal drift close to zero of an I-FOG with a quadrupole sensing coil wound by a PMF with 3.0 mm beat length and four different normalized temperature sensitivities close to zero drift.

In conclusion, the thermal drifts in IFOGs using PMFs strongly depend on the superposition or cancelation between pure Shupe error and phase error induced by thermal fluctuations of the fiber birefringence. The latter depends on the fiber materials and its fabrication processes, which makes the fiber design of PMFs fundamentally crucial for high-performance IFOGs. Our proposed model also shows that thermal drift in IFOGs using PMFs is affected by the sum of three terms: the thermal expansion of the fiber length, the temperature coefficient of the material refractive index and the thermal fluctuation of the fiber birefringence. The signs of the first two terms are positive when the temperature goes up, while the sign of the third term could be negative for a special fiber design which could introduce a new compensation method. The opposite sign would theoretically result in a zero value of

the drift when the birefringence term completely cancels pure Shupe errors by a specific fiber design and the design will be the main subject of our future work.

5. Conclusions

In this paper, we proposed a model of thermal drift for IFOGs with a sensing coil using high-birefringence PMFs. The model had discussed the effect of fiber birefringence for the first time to our knowledge. Using this new model, we have demonstrated that the temperature-induced stress effect originated from thermal fluctuation of fiber coatings can be suppressed by the intrinsic high birefringence in PMFs. This makes the suppression of thermal drift feasible for high performance IFOGs using PMFs. We also showed that the specific design of the modal birefringence and its temperature sensitivity for PMFs would cancel the pure Shupe error and contribute to a better performance towards zero drift.

Acknowledgement

This work is supported by EU Horizon2020 RISE Grant DAWN4IoE (No.778305).

References

1. H. C. Lefevre, The Fiber-Optic Gyroscope,2nd ed., Artech House, Boston/London, 2014, pp. 130.
2. D. M. Shupe, Thermally induced nonreciprocity in the fiber-optic interferometer, Appl. Opt.19 (1980)654-655.

3. S. Minakuchi, T. Sanada, N. Takeda, S. Mitani, T. Mizutani, Y. Sasaki, and K. Shinozaki, Thermal strain in light weight composite fiber-optic gyroscope for space application, J. Lightwave Technol. 33 (2015) 2658-2662.
4. H. C. Lefevre, The fiber-optic gyroscope: Challenges to become the ultimate rotation sensing technology, Opt. Fiber Technol. 19(2013) 828-832.
5. N. J. Frigo, Compensation of linear sources of non-reciprocity in Sagnac interferometers, Proc. SPIE0412(1983) 268-271.
6. F. Mohr, Thermo optically induced bias drift in fiber optical Sagnac interferometers, IEEE J. Lightwave Technol.14(1996)27-41.
7. Z. Li, Z. Meng, T. Liu, and X. S. Yao, A novel method for determining and improving the quality of a quadrupolar fiber gyro coil under temperature variations, Opt. Exp. 21 (2013) 2521-2530.
8. Z. Gao, Y. Zhang, G. Wang, and W Gao, Analysis and simulation for the thermal performance of the octupolar fiber coil, Opt. Eng. 53 (2014) 016114.
9. F. Mohrand F.Schadt, Bias error in fiber optic gyroscopes due to elastooptic interactions in the sensor fibers, in: Second European Workshop on Optical Fibre Sensors, Jose Miguel Lopez-Higuera, Brian Culshaw Ed, Proc. SPIE5502(2004) 410-415.
10. F. Mohr and F. Schadt, Rigorous treatment of fiber-environmental interactions in fiber gyroscopes,in: International Conference on Computational Technologies in Electrical and Electronics Engineering, IEEE REGION 8 SIBIRCON(2008)372-375.
11. S. Ogut, B. Osunluk, and E. Ozbay, Modeling of thermal sensitivity of a fiber optic gyroscope coil with practical quadrupole winding, in: Fiber Optic Sensors and

Applications XIV, S. Christopher, G. Pickrell, H. H, Du, E. Udd, J. J. Benterou, and A, Wang, Ed., Proc.SPIE10208(2017) 1020806.

12. W. Ling, X. Li, Z. Xu, Z. Zhang, and Y. Wei, Thermal effects of fiber sensing coils in different winding pattern considering both thermal gradient and thermal stress, Opt. Commun. 356 (2015) 290-295.
13. S. L. A. Carrara, B. Y. Kim, and H. J. Shaw, Bias drift reduction in polarization-maintaining fiber gyroscope, Opt. Lett. 12 (1987) 214-216.
14. D. Zhang, Y. Zhao, W. Fu, W. Zhou, C. Liu, X. Shu, and S. Che, Nonreciprocal phase shift caused by magnetic-thermal coupling of a polarization maintaining fiber optical gyroscope, Opt. Lett. 39 (2014) 1382-1385.
15. W. K. Burns, Phase error bounds of fiber gyro with polarization-holding fiber, J. Lightwave Technol. 4 (1986) 8-14.
16. J. N. Chamoun and M. J. F. Digonnet, Noise and bias error due to polarization coupling in a fiber optic gyroscope, J. Lightwave Technol. 33 (2015) 2839-2747.
17. G. B. Malykin and V. I. Pozdnyakiva, Ring Interferometry, Walter de Gruyter GmbH, Berlin/Boston, 2013, pp. 76.
18. M. P. Varnham, D. N. Payne, A. J. Barlow, and R. D. Birch, Analytic solution for the birefringence produced by thermal stress in polarization-maintaining optical fibers, J. Lightwave Technol. 1 (1983) 332-339.
19. P. L. Chu and R. A. Sammut, Analytical method for calculation of stresses and material birefringence in polarization-maintaining optical fiber, J. Lightwave Technol. 2 (1984) 650-662.

20. A. Kumar and A. Ghatak, Polarization of Light with Applications in Optical Fibers, SPIE Press, Bellingham, Washington, 2011, p. 177.
21. K. Mochizuki, Y. Namihira, and Y. Ejiri, Birefringence variation with temperature in elliptically cladded single-mode fibers, Appl. Opt. 21 (1982) 4223-4228.
22. D. Wong, Thermal stability of intrinsic stress birefringence in optical fibers, J. Lightwave. Technol. 8 (1990) 1757-1761.
23. F. Zhang and J. W. Y. Lit, Temperature and strain sensitivities of high-birefringence elliptical fibers, Appl. Opt. 31 (1992) 1239-1243.
24. K. S.Chiang, Temperature sensitivity of coated stress-induced birefringent optical fibers, Opt. Eng.36(1997)999-1007.
25. W. Urbabczyk, T. Martynkien, and W. J. Bock, Dispersion effects in elliptical-core highly birefringent fibers, Appl. Opt. 40 (2001) 1911-1920.
26. I. Abe, V. de Oliveira, and H. J. Kalinowski, Measurement of the birefringence temperature dependence in polarization maintaining fiber optics using Bragg gratings, Proc. SPIE. 8794 (2013) 8794-R-1.
27. S. Knudsen and K. Bbltekjar, Interferometric fiber-optic gyroscope performance owing to temperature-induced index fluctuations in the fiber: effect on bias modulation, Opt. Lett. 20 (1995) 1432-1434.
28. G. B. Hocker, Fiber-optic sensing of pressure and temperature, Appl. Opt. 18 (1979) 1445-1448.
29. M. Tateda, S. Tanaka, and Y. Sugawara, Thermal characteristics of phase shift in jacketed optical fibers, Appl. Opt.19(1980)770-773.

30. N.Lagakos, J. A.Bucaro, and J.Jarzynski, Temperature-induced optical phase shifts in fibers, Appl. Opt. 20 (1981) 2305-2308.

31. N. Lagakos, E. U. Schnaus, J. H. Cole, J. Jarzynski, and J. A. Bucaro, Optimizing fiber coatings for interferometric acoustic sensors, J. Quan. Eelec. 18 (1982) 683-689.

32. T. Musha, J. Kamimura, and M. Nakazawa, Optical phase fluctuations thermally induced in a single-mode optical fiber, Appl. Opt.21 (1982) 694-698.

33. L. S. Schuetz, J. H. Cole, J. Jarzynski, N. Lagakos, and J.A.Bucaro, Dynamic thermal response of single-mode optical fiber for interferometric sensors, Appl. Opt. 22 (1983) 478-483.

34. B. J. White, J. P. Davis, L. C. Bobb, H. D. Krumboltz, and D. C. Larson, Optical-fiber thermal modulator, J. Lightwave Technol. 5 (1987) 1169-1175.

35. W. Eickhoff, Temperature sensing by mode-mode interference in birefringent optical fibers, Opt. Lett. 6 (1981) 204-206.

36. T. Ito, Thermal hysteresis of phase retardation in polarization maintaining optical fibers, J. Lightwave Technol. 12 (1994) 1343-1347.

37. M. Fontaine, B. Wu, V. P. Tzolov, W. J. Bock, and W. Urbanczyk, Thermal stress effects on modal polarization properties of highly birefringent optical fibers, J. Lightwave Technol. 14 (1996) 585-591.

38. Z. Ding, Z. Meng, X. S. Yao, X. Chen, T. Liu, and M. Qin, Accurate method for measuring the thermal coefficient of group birefringence of polarization-maintaining fibers, Opt. Lett. 36 (2011) 2173-2175.

39. Y. H. Kim and K. Y. Song, Characterization of temperature-dependent birefringence in polarization maintaining fibers based Brillouin dynamic gratings, Proc. SPIE. 9655 (2015) 96553N.
40. P. Hlubina, M.Kadulova, D. Ciprian, and P. Mergo, Temperature sensing using the spectral interference of polarization modes in a highly birefringent fiber, Optics and Lasers in Engineering. 70 (2015) 51-56.
41. C. Kaczmarek, Measurement of the temperature sensitivity of modal birefringence of polarization maintaining optical fiber using a Sagnac Interferometer, IEEE Sensors Journal (2016) 3627-3632.
42. M. Wakaki, K. Kudo, and T. Shibuya, Physical Properties and Data of Optical Materials. CRC Press, New York, 2007, pp. 368.